PAPER

NJC
www.rsc.org/njc

A study of the effects of subunit pre-orientation for diarylpyrrole esters; design of new aryl-heteroaryl fluorescent sensors

John Killoran,[a] John F. Gallagher,[b] Paul V. Murphy[a] and Donal F. O'Shea*[a]

[a] *Centre for Synthesis and Chemical Biology, Conway Institute, Department of Chemistry, University College Dublin, Belfield, Dublin 4, Ireland. E-mail: donal.f.oshea@ucd.ie; Tel: +353-(0)1-7162425*

[b] *School of Chemical Sciences, Dublin City University, Dublin 9, Ireland*

Received (in Durham, UK) 31st May 2005, Accepted 11th August 2005
First published as an Advance Article on the web 7th September 2005

The synthesis, single crystal X-ray structures, spectroscopic properties and molecular mechanics calculations of three systematically substituted 3,5-diaryl-1*H*-pyrrole-2-carboxylic acid ethyl esters **1a–c** are described. The goal is to develop design principles for the generation of new class of fluorescent switches constructed from an aryl-heteroaryl architecture containing a virtual (C_0) spacer. The spectroscopic effects of the electron donor *p*-dimethylamino substituent of **1b** and the combined steric and electron donor impact of the *o*-methyl-*p*-dimethylamino groups of compound **1c** were investigated to determine the required structural motifs to achieve orthogonal pre-orientation of the sensor subunits.

Introduction

In spite of its long history the development of molecular based fluorescent sensors continues to be a very active area of research.[1] Specifically, in the field of molecular biology the use of high sensitivity fluorescence detection has become a common tool for gaining a greater understanding of the molecular processes in biological systems.[2] The success of this strategy is underlined by the increasing number of assay systems that are based upon a molecular recognition event coupled with fluorescence output. The design of fluorescent probes, with the fluorescence switching properties controlled by an excited state electron transfer mechanism, typically adopts a modular building block approach such as the receptor–spacer–fluorophore architecture.[3] The function of the receptor is to detect the targeted analyte, whereas the role of the fluorophore is to quantify and communicate this detection to the observer. The purpose of the spacer unit, the least structurally complex component, is to covalently link the fluorophore to the receptor whilst keeping the ground state electronic systems of the receptor and the fluorophore disconnected. The spacer component most commonly comprises a saturated methylene unit (C_1 spacer), which effectively decouples the system (model A, Fig. 1).[4] The electronic separation of receptor and fluorophore can also be accomplished by a virtual spacer (C_0), though this approach is significantly less exploited (model B, Fig. 1).[3a,5] When using a virtual spacer, the receptor module is covalently linked directly to the fluorophore but their electronic systems remain disconnected as a result of a forced orthogonal conformation between the receptor and fluorophore. The σ bond framework linking the receptor and fluorphore subunits can cause a twist of the components away from co-planarity. If a near orthogonal conformation exists, the electron system of the receptor remains decoupled from that of the fluorophore due to restricted π-orbital overlap (Fig. 1, model B). This approach is particularly suited to biaryl systems as they are characterised by an inherent restricted flexibility about the single biaryl bond and switching efficiency can often be controlled by the degree of interannular twist.

A further design can comprise an integrated, or intrinsic, fluorophore-receptor approach in which there is no electronic separation of receptor and fluorophore and switching is modulated by an internal charge transfer (ICT) process as depicted by model C (Fig. 1). Recently combination sensors comprising models A and C have been reported as potential two-dimensional fluorescent sensors.[6]

We are currently interested in developing new visible red and near infrared (NIR) sensors based upon the BF_2 chelated tetraarylazadipyrromethene fluorophore (Fig. 2). We have recently reported this chromophore class to have highly sought after absorption and emission characteristics in the 650–750 nm region of the spectrum which could facilitate their application as *in vitro* and *in vivo* biomedical diagnostic agents.[7] NIR dyes are suitable for such applications due to efficient penetration of light through tissue and the low auto-fluorescence of endogenous chromophores in this spectral region. Our current design approach is to adopt an aryl-heteroaryl subunit pre-orientation approach (model B) using a substituted aryl ring containing the receptor linked to a pyrrole ring of the fluorophore.

In the course of this work we have generated an intermediate system for study, the 3,5-diaryl-1*H*-pyrrole-2-carboxylic acid

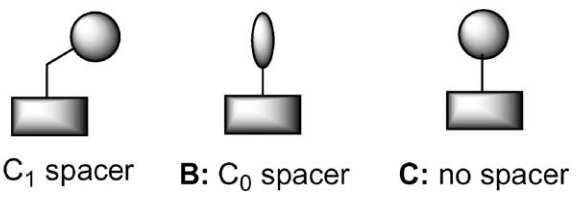

Fig. 1 Schematic of fluorescent sensor designs. Rectangle = fluorophore; circle = receptor; oval = orthogonal receptor.

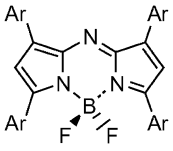

Fig. 2 BF_2 Chelated tetraarylazadipyrromethenes.

DOI: 10.1039/b507669b

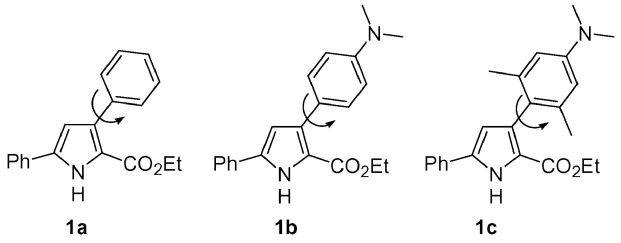

Fig. 3 3,5-Diaryl-1*H*-pyrrole-2-carboxylic acid ethyl esters.

ethyl esters **1a–c** which would assist in the overall design of our NIR analogues and has revealed interesting properties of their own (Fig. 3). A study of these compounds has shown their potential to determine the effects of subunit pre-orientation in an aryl-heteroaryl system and serve as useful design tools for the more complex BF_2 chelated tetraarylazadipyrromethene systems.

Results and disscussion

Synthesis

To pursue our synthetic strategy we required a robust versatile synthesis of 2,4-diarylpyrroles. Despite their synthetic importance, direct methods for making 2,4-diarylpyrroles are limited especially if two different aryl substituents are required. Routes to symmetrical substituted 2,4-diarylpyrroles include SmI_2 mediated reductive dimerisation of phenacyl azides,[8] reaction of hexacarbonylmolybdenum with 3-aryl-2*H*-azirines,[9] and Grignard mediated dimerization of acetophenone oximes.[10] Rhodium and zirconium catalysed reaction of alkynes, amines and carbon monoxide have been reported as procedures to unsymmetrically substituted derivatives but these methods require high pressure CO conditions.[11,12] Our approach followed a literature methodology which exploited a reductive cyclisation of electron deficient γ-nitroketones with formamidinesulfinic acid.[13] The starting point for our synthesis were the 1,3-diarylpropenones (chalcones) **2**. Compound **2a** was commercially available and **2b–c** were synthesised by an aldol/dehydration reaction of the corresponding aldehyde and acetophenone. The generation of **3** was achieved by the addition of nitroacetic acid ethyl ester to 1,3-diarylpropenones **2**. Reductive cyclization of **3** with formamidinesulfinic acid provided the ester substituted diarylpyrroles **1a–c** in moderate yields (Scheme 1).

X-Ray crystallographic study

Compounds **1a–c** were examined by single crystal X-ray diffraction in order to determine the nature of the inter-planar angle between the aryl-pyrrole rings and compare their molecular and crystal structures. In addition, the solid state structures would facilitate a correlation of structural differences with data available from spectroscopic characteristics and molecular mechanics calculations and aid in the general design of future sensors. Crystals were grown by the slow room temperature evaporation of ethanolic solutions of each compound. Compound **1a** crystallised in the monoclinic system, space group $P2_1/c$ (No. 14) ($Z' = 1$) while both derivatives **1b** ($Z' = 2$, two independent molecules A and B per asymmetric unit) and **1c** ($Z' = 1$) crystallised in the triclinic system ($P\bar{1}$, No. 2)†.

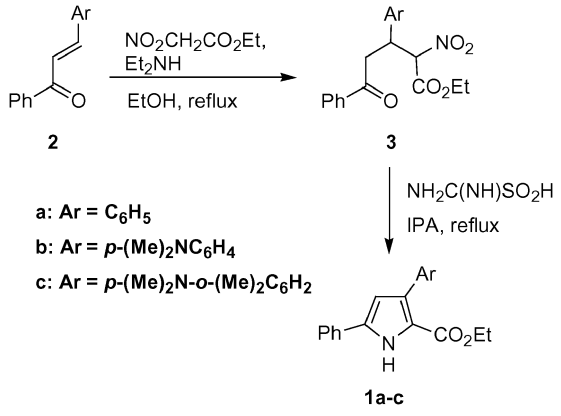

Scheme 1

The major difference observed between the three systems was the inter-planar angle between the C3 substituted aromatic ring {C31,···,C36} and the central pyrrole ring {N1,C1···,C4} which varies from 43.42(7)° in **1a** to 32.98(10)/37.40(7)° (A/B) in **1b** to the almost orthogonal 82.87(4)° in **1c** (Fig. 4, Table 1). This indicates that the inclusion of *ortho* methyl groups in **1c** would be a more effective design for achieving an electronically disconnected system between the aryl-heteroaryl system when compared to **1b**.

Further analysis of the three structure reveals that for the unsubstituted phenyl ring at C1, the inter-planar angle with the central pyrrole is 25.39(9)° in **1a**; 17.23(12)/30.80(9)° for **1b** and 4.10(9)° for **1c**. As expected, a smaller variance in this inter-planar angle was found between the three systems. However, the orientation of this phenyl ring does have an important secondary role to play in the intermolecular hydrogen bonding in the solid state (discussed later).

At the substituted pyrrole carbon atom C3, the C4–C3–C31 angles are 130.73(15)°, 131.48(19)/131.34(18)° and 129.06(11)° Å in **1a**, **1b** and **1c** respectively, a difference of 2.5°. In contrast at C4 for the related C3–C4–C5 angles there is a larger difference of 4° (Table 1). This can be explained by the substitution pattern at C3 and C4, whereby the increasing steric bulk of the substituted phenyl ring along the **1a–c** series influences the bond angles at C4. In **1c**, the orthogonal orientation of the aryl ring relative to the pyrrole facilitates the C4–C3–C31 and C3–C4–C5 angles to close relative to **1a** and **1b**. In contrast the differences in the internal C2–C3–C4/C3–C4–N1 angles are, however, only 0.4/0.6° between **1a–c**. The *ipso* angles in the substituted phenyl group at C3, *e.g.* C32–C31–C36, vary as 118.37(18)°, 116.16(19)°/116.08(18)° and 119.13(10)°, a 3° difference in the substituted aromatic rings $-C_6H_5$, $-C_6H_4(NMe_2)$ and $-C_6H_2(Me)_2(NMe_2)$. The smaller angle in **1b** derives from the influence of the NMe_2 moiety as it is intermediate in structure between **1a** and **1c**.

Bond length analysis of the pyrrole ring in **1a–c** reveals that there are few significant differences between the three structures (Table 2). But analysis of the aromatic C–C bond lengths of both the substituted and unsubstituted aryl rings in **1b** show that the two shortest C–C bonds are the C32–C33/C35–C36 pair with 1.376(3)/1.376(3) Å and 1.383(3)/1.378(3) Å in molecules A/B, in comparison to the range of 1.388(3) to 1.397(3) Å for the eight other C–C distances in both C_6 rings. No significant C–C differences are discernible in the other four aromatic rings of either **1a** or **1c**. The C–NMe_2 bond lengths in **1b** are 1.389(3)/1.390(3) Å with twist angles of 6.1(3)°/14.80(12)° between the Me_2N and C_6 planes. This provides supporting evidence for some delocalisation in **1b** along the *para*-substituted $-C_6H_4-NMe_2$ moiety.

Hydrogen bonding and crystal engineering studies continue to attract much interest in a diverse range of areas of structural science with potential applications in pharmaceuticals, polymorphism, medicinal chemistry, materials for optical/switching devices, designer supramolecular systems and controlling crystal growth.[14] Of increasing importance is the nature of the weak interaction *e.g.* C–H···O, C–H···π(arene) and how these interactions can be manipulated and controlled in the 3-D crystal structure.[15] In our series each pyrrole derivative associated through $_{(pyrrole)}N–H\cdots O{=}C_{(ester)}$ hydrogen bonding into dimeric units resulting in the formation of a hydrogen

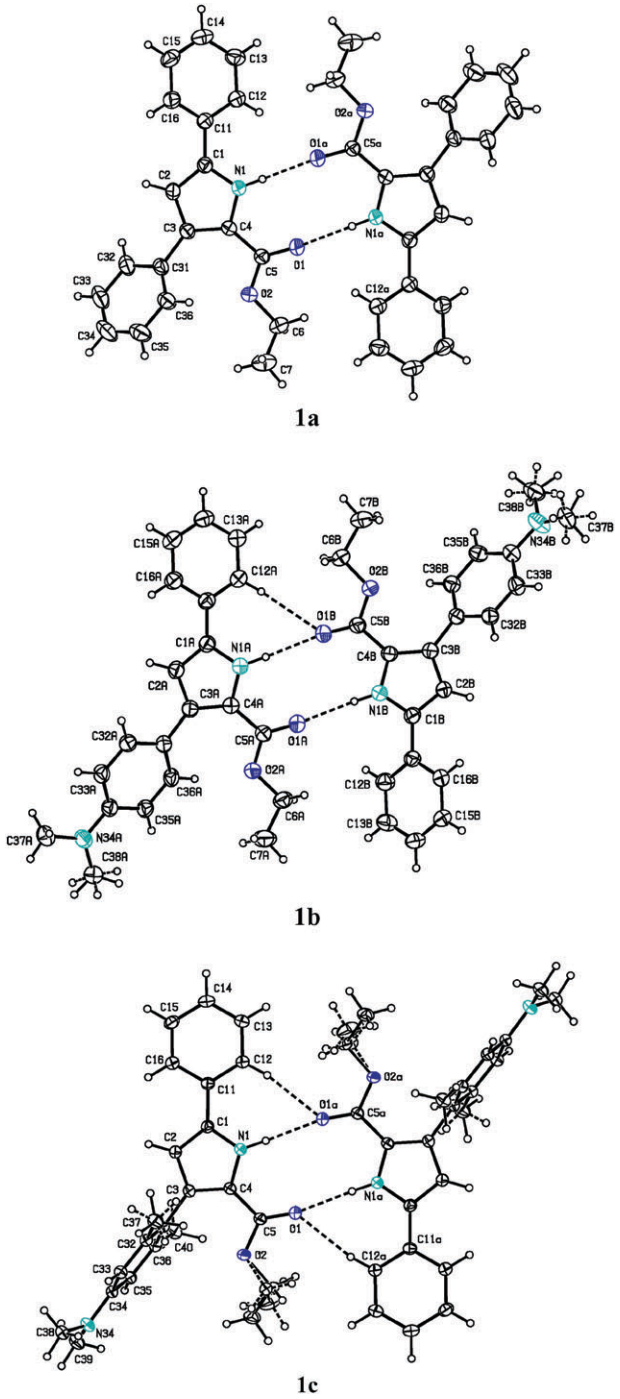

Fig. 4 ORTEP diagrams of **1a**, **1b** and **1c** with displacement ellipsoids depicted at the 30% probability level. Hydrogen bonds and contacts are depicted with dashed lines. **1a** and **1c** with a symmetry equivalent molecule at −x, −y, −z and 1 − x, 1 − y, 1 − z, respectively.

bonded ring with graph set $R_2^2(10)$, (Fig. 5).[16] The strong intermolecular N–H···O hydrogen bonding is centrosymmetric in **1a** and **1c** with one molecule per asymmetric unit, whereas it comprises two independent A/B molecules in the form of a hydrogen bonded dimer in **1b** ($Z = 4$ in space group $P\bar{1}$, No. 2†). The hydrogen bonding N···O distances differ from 2.9480(18) Å in **1a**; 3.068(2) and 2.995(2) Å in **1b** to 2.9888(13) Å in **1c**. An overview of the hydrogen bonding is represented in Fig. 5 with full details presented in Table 3.

The crystal structure of **1a** shows that there are no additional intermolecular hydrogen bonding interactions assisting the N–H···O=C hydrogen bonded ring formed between each molecule in the dimeric unit (Table 3). In the crystal structure of **1b** a C–H···O interaction is present in tandem with the

Table 1 Selected bond angles for **1a–c** in [°]

	1a	1b[a]	1c
Aryl–pyrrole twist	43.42(7)	32.98(10)/37.40(7)	82.87(4)
N1–C1–C2	106.77(14)	106.50(18)/107.14(17)	106.96(10)
N1–C4–C3	107.70(14)	107.90(18)/107.99(17)	108.29(10)
C1–N1–C4	110.27(14)	110.34(18)/109.87(17)	109.76(9)
C1–C2–C3	109.32(14)	109.72(19)/109.35(18)	109.00(10)
C2–C3–C4	105.93(14)	105.53(18)/105.62(17)	105.97(10)
C3–C4–C5	134.69(15)	135.3(2)/134.32(18)	131.37(11)
C4–C3–C31	130.73(15)	131.48(19)/131.34(18)	129.06(11)
C5–O2–C6	118.13(14)	116.29(17)/117.62(17)	Disordered
C32–C31–C36	118.37(18)	116.16(19)/116.06(18)	119.13(10)

[a] Two independent molecules A/B are present.

Table 2 Selected bond lengths for **1a–c** in [Å]

	1a	1b[a]	1c
N1–C1	1.358(2)	1.361(3)/1.361(3)	1.3631(15)
N1–C4	1.373(2)	1.375(3)/1.378(2)	1.3758(14)
C1–C2	1.379(2)	1.378(2)/1.379(3)	1.3873(16)
C2–C3	1.402(2)	1.407(3)/1.408(3)	1.4057(16)
C3–C4	1.394(2)	1.394(3)/1.399(3)	1.3913(16)
C4–C5	1.454(2)	1.452(3)/1.449(3)	1.4525(17)
C1–C11	1.466(2)	1.462(3)/1.467(3)	1.4678(16)
C3–C31	1.483(2)	1.486(3)/1.477(3)	1.4860(15)
N34–C34	—	1.389(3)/1.390(3)	1.3894(15)

[a] Two independent molecules A/B are present.

N–H···O=C hydrogen bonded ring system thus generating an additional hydrogen bonded motif with graph set $R_2^1(7)$. In the A/B hydrogen bonded dimeric unit in **1b** the intramolecular inter-planar angles that the C1-phenyl ring makes with the pyrrole moiety are 17.23(12)° (A) and 30.80(9)° (B).

The former (a reduction from 25.39(9)° in **1a**) enables the formation of a C12A–H12A···O1B interaction with C12A···O1B, 3.445(3) Å and H12A···O1B 2.57 Å (C–H···O angle of 157°), but the phenyl/pyrrole angle difference of 15° between molecules A and B precludes the formation of a second and reciprocal C12B–H12B···O1A interaction (Fig. 6). The contact data from B → A are 3.616(3) Å, 2.96 Å and 129°, thus ruling out this possible interaction being considered even as a contact. There are no π-stacking or C–H···π (arene) interactions of note in **1b** apart from a myriad of contacts and van der Waals interactions.

In **1c** the centrosymmetric hydrogen bonded dimer contains two C–H···O additional interactions involving C12–H12···O1^{ii}/C12–H12^{ii}···O1 as a centrosymmetric related pair, in contrast to one C-H···O in **1b** and none in **1a** (Table 3). Although the interplanar (perpendicular) distances are reasonably short between adjacent dimers the planes do not align to give an overlapping π-stack in the crystal structure. The distance data for **1c** are C12···O1^{ii} 3.3707(16) Å, H12···O1^{ii},

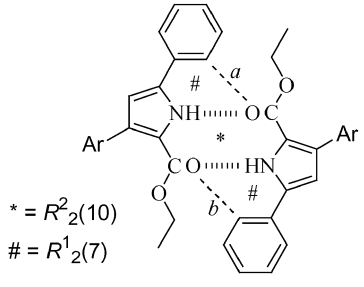

a = **1b** and **1c**; *b* = **1c** only

Fig. 5 Schematic drawing of the intermolecular hydrogen bonding within the dimeric species in **1a–c**.

Table 3 Intermolecular hydrogen bonding, contact and distance parameters for **1a–c**

	1a	**1b**[a]	**1c**
N1···O1^{i} (Å)	2.9480(18)	3.068(2)/2.995(2)	2.9888(13)
H1···O1^{i} (Å)	2.128(19)	2.15(2)/2.09(2)	2.095(15)
N1–H1–O1^{i} (°)	162.6(16)	174(2)/176.4(19)	170.3(14)
C12···O1^{i} (Å)	3.614(2)	3.445(3), 3.616(3)	3.3707(16)
H12···O1^{i} (Å)	3.01	2.57, 2.96	2.43
C12–H12···O1^{i} (°)	124	157, 129	169
C36···O2 (Å)	2.928(2)	2.932(2)/2.910(3)	3.4897(18)
H36···O2 (Å)	2.54	2.44/2.47	2.87 (H40C)
C36–H36···O2 (°)	105	113/109	122
C_6H_5/pyrrole (°)	25.39(9)	17.23(12)/30.80(9)	4.10(9)
Subs.C_6/pyrrole[b] (°)	43.42(7)	32.98(10)/37.40(7)	82.87(4)
Me_2N/C6 (°)	—	6.1(3)/14.80(12)	17.83(8)

[a] Two independent molecules A/B are present. [b] The substituted {C31,···,C36} ring system in all three derivatives. i = symmetry operator −x, −y, −z in **1a**, no symmetry operator in **1b**; 1 − x, 1 − y,1 − z in **1c**.

2.43 Å and C12–H12···O1^{ii}, 169° which are significantly shorter than **1b**.

The overall trend in the hydrogen bonding (disregarding the effects of the overall crystal packing) is the presence of the hydrogen bonded N–H···O=C ring system in all three crystal structures and the presence of additional 0, 1, 2 $_{ortho}$C–H···O=C interactions augmenting the central N–H···O=C ring on progression from the phenyl **1a**, 4-substituted aryl **1b** to the 2,4,6-substituted aryl ring system **1c**. The known tendency for the strongest hydrogen bond donor to pair with the strongest acceptor is observed for **1a** to **1c** with additional weaker C–H···O interactions supplementing this interaction. In a structurally related system we have previously reported dipyrromethanes where only N–H···π(pyrrole) interactions are observed in the absence of stronger hydrogen bond donors/acceptors.[17]

There are no close pyrrole analogues of **1a–c** available on the Cambridge Structural Database (CSD) reported to date using a search for the central pyrrole core with two C_6 aromatic rings attached. However, an example VUGDEG,[11,18] 5-methyl-*N*,3-diphenylpyrrole-2-carboxamide has the general substitution pattern of three carbon atoms replacing three of the H atoms on a pyrrole ring system, while XETXID,[19] ethyl 3-methyl-5-phenylpyrrole-2-carboxylate differs from **1a** by replacing a phenyl with a methyl group. This study of **1a–c** highlights that functional groups at remote positions in a molecular system can introduce subtle differences in both the molecular and crystal structures as manifested in bond length/angles differences and overall intermolecular hydrogen bonding.

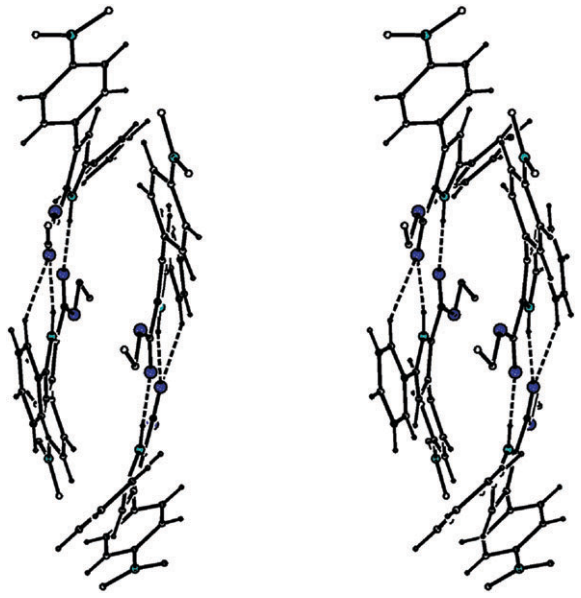

Fig. 6 Stereoview diagram of a pair of hydrogen bonded dimers in **1b**. The H atoms on the CH_3 and CO_2Et groups have been removed for clarity.

Spectroscopic study

The steady state photophysical properties of **1a–c** are shown in Fig 7. The absorption spectrum of **1a** exhibited two distinct bands with little solvent dependency between non-polar cyclohexane and polar acetonitrile. The fluorescence spectrum of **1a** shows slight solvent dependency with a variance of 6 nm for the emission maximum in cyclohexane and acetonitrile with Stoke shifts of 44 and 56 nm respectively (Table 4).

The absorption spectrum of **1b** displayed a single band again with little solvent effect. But in contrast to **1a** the fluorescence

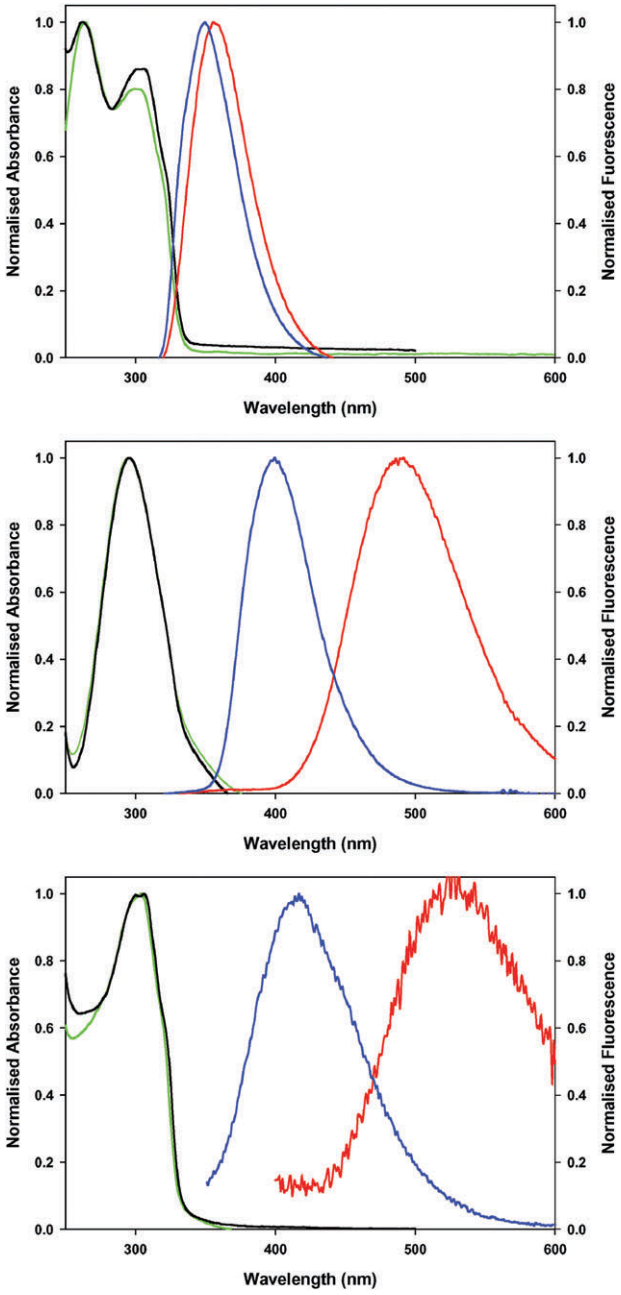

Fig. 7 Normalised absorption and fluorescence spectra of **1a** (top), **1b** (middle), **1c** (bottom) in cyclohexane (black, blue) and acetonitrile (green, red).

Table 4 Spectroscopic data for **1a–c**[a]

	Solvent	λ_{max} abs [nm]	λ_{max} flu [nm]	Stoke shift [nm]
1a	C_6H_{12}	262/306	350	44
1a	CH_3CN	263/300	356	56
1b	C_6H_{12}	296	400	104
1b	CH_3CN	295	492	197
1c	C_6H_{12}	306	417	111
1c	CH_3CN	304	524	220

[a] Room temperature.

spectrum showed a pronounced solvatochromic effect with larger Stokes' shifts. The wavelength of emission maxima in cyclohexane (400 nm) and acetonitrile (492 nm) varied by 92 nm with the Stokes' shift increasing from 104 nm to 197 nm due to the solvent polarity change. This would be indicative of a high charge-transfer character of the emitting state. A similar but even more pronounced effect was observed for the fluorescence spectra of **1c**. The emission maximum in cyclohexane was at 417 nm with a larger red shift to 524 nm in acetonitrile. The increase in Stoke shifts to 111 nm in cyclohexane and 220 nm in acetonitrile is indicative of an increased electronic decoupling in **1c**. In conjunction with the red shifts, broadening of the bands was also observed and in the case of **1c** a significant diminishing of fluorescence intensity in acetonitrile. These spectral characteristics are similar in some respects to those reported for other reported dimethylamino substituted CT sytems.[20] The characteristics of the fluorescence spectra of **1b–c** in polar solvent indicates that their fluorescence state is different from the originally locally-excited (LE) state. The increasing Stokes' red shift with increasing solvent polarity implies that **1b–c** in the fluorescent state has a large dipole moment which is most likely the intramolecular charge transfer state. One could propose that from a comparison of absorption and fluorescence characteristic for the series **1a–c** that **1a** emits from a less polar LE state whereas **1b–c** emit either from a CT state or a combination of CT and LE. While aromatic amino esters have been reported as having solvent dependant emissions it is interesting to observe such characteristics from a pyrrole ester. A previously reported examples exploiting pyrrole units in a donor–acceptor system used the pyrrole as the donating group.[21] As such the unique architecture of this system coupled with its interesting spectral properties warrants a further in depth photophysical study.

Computational study

The coordinates from the crystal structures **1a–c** provided the starting structures that were used in the conformational analysis. The dihedral angle (φ) between the C3 substituted aromatic ring and the pyrrole ring was varied by 1° increments using the dihedral driving feature in Macromodel 8.5 and the energy calculated after minimization at each incremental stage using the MM2 force field in the gas phase.[22] The results obtained were plotted as shown in Fig. 8 which provided the calculated ground state twist potential of **1a–c**.

All atoms were constrained during the calculation except for the rotating aromatic group at the pyrrole C-3 position and energy minima were calculated at one-degree intervals. **1a** and **1b** gave similar results with an energy minimum between 38–44° and 33–38° respectively. This was in good agreement with the experimental C3 aryl-pyrrole inter-planar angle from their crystal structures. Both **1a** and **1b** showed a significant barrier to rotation for $\varphi = 90°$ of 11.6 kJ mol^{-1} and 13 kJ mol^{-1} respectively. In contrast **1c** showed a significantly lower barrier (2 kJ mol^{-1}) to rotation about the 60–120° range but a large barrier (60 kJ mol^{-1}) to both rings becoming co-planar, again in agreement with the solid-state structure. The close agreement of the results of this computational method with our experimental crystallographic data suggests that this would be a powerful predictive tool for other systems.

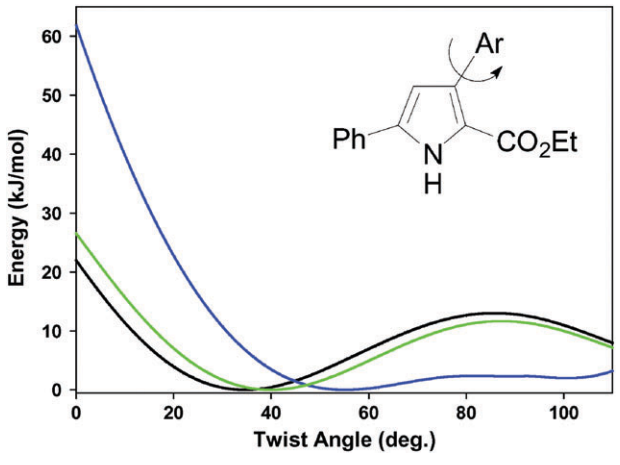

Fig. 8 Ground state twist potential (φ) of **1a** (green) **1b** (black) and **1c** (blue) derived from MM2 force field in the gas phase.

Conclusion

We have synthesised a series of diaryl-pyrroles and characterised key parameters to determine their suitability for incorporation into fluorescent sensors designed upon the virtual C_0 spacer principles. Solution, solid state and computational evidence for the key characteristics of these systems provides an excellent platform for the design of future more complex visible red and NIR analogues.

Experimental

General

^{1}H NMR spectra were recorded on a Varian FT spectrometer at 300 MHz and ^{13}C NMR spectra at 75 MHz, in $CDCl_3$ with tetramethylsilane as the internal standard. All chemical shifts are quoted in δ (ppm) and coupling constants in Hz. Melting points were determined on a Reichert Thermovar melting point platform and are uncorrected. Mass spectral analyses were performed on a Micromass Quattro Micro. IR spectra were recorded on a Mattson Instruments Galaxy series FT-IR 3000 spectometer. Absorption spectra were recorded on a Varian Cary 50 UV-visible spectrophotometer. Fluorescence spectra were recorded on a Cary Eclipse spectrofluorometer. The microanalytical laboratory, University College Dublin, carried out the elemental analyses.

4-Dimethylamino-2,6-dimethylbenzaldehyde. $POCl_3$ (6.85 g, 44.7 mmol) was added dropwise over 20 minutes to DMF (13.06 g, 179 mmol) that was cooled on an ice bath. The solution was allowed to stir for 30 minutes after which it was added dropwise over 30 minutes to 3,5-dimethylphenyldimethylamine (20 g, 134 mmol) under nitrogen and cooled on an ice bath. The mixture was stirred at room temperature for 8 hours during which time a brown solid formed. Ice (120 g) was added and the reaction mixture was adjusted to pH 7 with 33% NaOH solution (15 mL). The mixture was extracted with ether (5 × 100 mL), the organic layer was separated, dried over sodium sulfate and the solvent evaporated. The excess amine (12.5 mL recovered) was distilled off and the product was isolated from the resulting residue after recrystallisation from petroleum spirits (40–60) as a white solid (5.53 g, 70%); mp 84–85 °C (lit mp 83 °C).[23] ^{1}H NMR (300 MHz, $CDCl_3$) δ: 10.35 (s, 1H), 6.30 (s, 2H), 3.03 (s, 6H), 2.59 (s, 6H); ^{13}C NMR (75 MHz, $CDCl_3$) δ: 190.7, 153.1, 144.4, 121.7, 112.2, 40.0, 21.8; IR (KBr disc): $\upsilon_{C=O}$ 1666 cm^{-1}; ES-MS (m/z) calcd. for

$C_{11}H_{16}N$: 178.0 $(M + H)^+$; found: 178.1; Anal. calcd. for $C_{11}H_{15}N$: C, 74.54; H, 8.53; N, 7.90; found: C, 74.42; H, 8.54; N, 7.76.

3-(4-Dimethylaminophenyl)-1-phenylpropenone (2b). 4-Dimethylaminobenzaldehyde (10 g, 67 mmol), 1-phenylethanone (8.05 g, 67 mmol) and four NaOH pellets were dissolved in methanol (100 mL) and stirred at room temperature for 24 hours during which time a precipitate formed. The precipitate was isolated by filtration and washed with cold methanol to give the product **2b** as a bright yellow solid, (14.1 g, 84%), mp 111–112 °C (lit. m.p. 110–111 °C).[24] ^{1}H NMR (300 MHz, $CDCl_3$) δ: 7.98–8.02 (m, 2H), 7.79 (d, $J = 15.5$ Hz, 1H), 7.43–7.56 (m, 5H), 7.32 (d, $J = 15.5$ Hz, 1H), 6.64–6.69 (m, 2H), 3.00 (s, 6H); ^{13}C NMR (75 MHz, $CDCl_3$) δ: 190.8, 152.3, 146.0, 139.3, 132.3, 130.6, 128.7, 128.5, 122.9, 117.1, 112.0, 40.3; IR (KBr disc): $\upsilon_{C=O}$ 1649 cm^{-1}; ES-MS (m/z) calcd. for $C_{17}H_{18}NO$: 250.0 $(M + H)^+$; found 252.1; Anal. calcd. for $C_{17}H_{17}NO$: C, 81.24; H, 6.82; N, 5.57; found: C, 80.95; H, 6.82; N, 5.49%.

3-(4-Dimethylamino-2,6-dimethylphenyl)-1-phenylpropenone (2c). 4-Dimethylamino-2,6-dimethylbenzaldehyde (4.5 g, 25 mmol), 1-phenylethanone (3 g, 25 mmol) and four NaOH pellets were dissolved in methanol (50 mL) and stirred at room temperature for 24 hours during which time a precipitate formed. The precipitate was isolated by filtration and washed with cold methanol to give the product **2c** as a bright yellow solid, (3.8 g, 54%), mp 93–95 °C. ^{1}H NMR (300 MHz, $CDCl_3$) δ: 8.11 (d, $J = 15.8$ Hz, 1H), 7.97–7.99 (m, 2H), 7.45–7.55 (m, 3H), 7.14 (d, $J = 15.8$ Hz, 1H), 6.44 (s, 2H), 2.99 (s, 6H), 2.48 (s, 6H); ^{13}C NMR (75 MHz, $CDCl_3$) δ: 191.0, 150.8, 143.6, 140.4, 139.2, 132.4, 128.7, 128.6, 123.2, 122.1, 112.6, 40.3, 22.9; IR (KBr disc): $\upsilon_{C=O}$ 1654 cm^{-1}; ES-MS (m/z) calcd. for $C_{19}H_{22}N$: 280.0 $(M + H)^+$; found: 280.1; Anal. calcd. for $C_{19}H_{21}N$: C, 81.68; H, 7.58; N, 5.01; found C, 81.75; H, 7.63; N, 5.31%.

2-Nitro-5-oxo-3,5-diphenylpentanoic acid ethyl ester (3a). Compound **2a** (10 g, 48 mmol) was dissolved in ethanol (80 mL), diethylamine (0.35 g, 4.8 mmol) and nitro-acetic acid ethyl ester (3.33 g, 25 mmol) were added, and the reaction was heated under reflux for 18 hours. The reaction mixture was allowed to cool to room temperature, acidified with 50% acetic acid solution (5 mL), diluted with water (20 mL) and the resulting precipitate was isolated by filtration. Recrystallisation from ethanol gave the product **3a** as a white solid (14.3 g, 87%), m.p. 111–113 °C (lit. m.p. 116–117 °C).[25] ^{1}H NMR (300 MHz, $CDCl_3$) δ: 7.86–7.89 (m, 2H), 7.51–7.57 (m, 1H), 7.4–7.45 (m, 2H), 7.22–7.32, (m, 5H), 5.61, 5.54, (each d, $J = 9.5$, 8.5 Hz, 1H), 4.45–4.55 (m, 1H), 4.02–4.29 (m, 2H), 3.45–3.74 (m, 2H), 1.22, 1.06 (each t, $J = 7.2$, 7.2 Hz, total 3H); ^{13}C NMR (75 MHz, $CDCl_3$) δ: 196.6, 196.5, 163.9, 163.4, 138.2, 137.2, 136.7, 133.7, 133.6, 129.1, 129.1, 128.9, 128.7, 128.3, 128.3, 128.2, 91.8, 91.7, 63.4, 63.2, 42.1, 41.7, 41.0, 40.7, 13.9, 13.8; IR (KBr disc): $\upsilon_{C=O}$ 1751, $\upsilon_{C=O}$ 1682 cm^{-1}; ES-MS (m/z) calcd. for $C_{19}H_{20}NO_5$: 342.0 $(M + H)^+$; found: 342.1; Anal. calcd. for $C_{19}H_{19}NO_5$: C, 66.85; H, 5.61; N, 4.10. Found C, 66.79; H, 5.61; N, 4.11%.

3-(4-Dimethylaminophenyl)-2-nitro-5-oxo-5-phenylpentanoic acid ethyl ester (3b). Compound **2b** (14.1 g, 56 mmol) was dissolved in ethanol (100 mL), diethylamine (0.41 g, 5.6 mmol) and nitro-acetic acid ethyl ester (11.22 g, 84 mmol) were added, and the reaction was heated under reflux for 24 hours. The reaction mixture was allowed to cool to room temperature, acidified with 50% acetic acid solution (15 mL), diluted with water (100 mL) and the resulting precipitate was isolated by filtration. Recrystallisation from ethanol gave the product **3b** as a white solid (15.8 g, 74%), mp 102–104 °C. ^{1}H NMR (300 MHz, $CDCl_3$) δ: 7.86–7.90 (m, 2H), 7.49–7.55 (m, 1H), 7.38–7.44 (m, 2H), 7.10–7.17 (m, 2H), 6.58–6.62 (m, 2H), 5.55, 5.49 (each d, $J = 9.4$, 8.5 Hz, total 1H), 4.35–4.43 (m, 1H), 4.04–4.28, (m, 2H), 3.36–3.68 (m, 2H), 2.87 (s, 6H), 1.22, 1.08 (each t, $J = 7.2$, 7.2 Hz, total 3H); ^{13}C NMR (75 MHz, $CDCl_3$) δ: 196.9, 163.6, 150.4, 136.8, 133.5, 129.3, 129.0, 128.8, 128.3, 124.2, 112.8, 92.2, 92.1, 63.3, 63.0, 41.4, 41.3, 41.1, 40.9, 40.5, 13.9; IR (KBr disc): $\upsilon_{C=O}$ 1743, $\upsilon_{C=O}$ 1683 cm^{-1}; ES-MS (m/z) calcd. for $C_{21}H_{25}N_2O_5$: 385.0 $(M + H)^+$; found: 385.2; Anal. calcd. for $C_{21}H_{24}N_2O_5$: C, 65.61; H, 6.29; N, 7.29; found C, 65.47; H, 6.28; N, 7.29%.

3-(4-Dimethylamino-2,6-dimethylphenyl)-2-nitro-5-oxo-5-phenylpentanoic acid ethyl ester (3c). Compound **2c** (0.68 g, 2.43 mmol) was dissolved in ethanol (15 mL), diethylamine (0.04 g, 0.41 mmol) and nitro-acetic acid ethyl ester (0.54 g, 4.1 mmol) were added, and the reaction was heated under reflux for 24 hours. The reaction mixture was allowed to cool to room temperature, acidified with 25% acetic acid solution (2 mL) and diluted with water (10 mL) which resulted in an oil. The water was removed by evaporation and the resulting residue was taken up in CH_2Cl_2 and washed with a saturated sodium bicarbonate solution (2 × 25 mL). The organic layer was separated, dried over sodium sulfate and evaporated to dryness. Purification by dry flash column chromatography on silica eluting with hexane/ether (2 : 1) gave the unreacted starter first (0.32 g) and the product **3c** second as a straw yellow oil (0.2 g, 20%). ^{1}H NMR (300 MHz, $CDCl_3$) δ: 7.83–7.90 (m, 2H), 7.51–7.55 (m, 1H), 7.39–7.46 (m, 2H), 6.32 (s, 1H), 6.31 (s, 1H), 5.78, 5.69 (each d, $J = 11.7$, 11.2 Hz, total 1H), 4.99–5.16 (m, 1H), 3.89–4.15 (m, 2H), 3.35–3.73 (m, 2H), 2.87, 2.85 (each s, total 6H), 2.50, 2.46, 2.40, 2.37 (each s, total 6H), 1.20, 0.92 (each t, total 3H); ^{13}C NMR (75 MHz, $CDCl_3$) δ: 196.9, 164.2, 163.3, 149.6, 149.4, 136.8, 133.3, 133.1, 128.3, 122.7, 120.9, 114.1, 114.0, 113.1, 113.0, 90.7, 90.3, 63.2, 62.5, 36.1, 35.1, 41.4, 40.9, 40.3, 40.2, 13.7, 13.3; IR (CH_2Cl_2): $\upsilon_{C=O}$ 1750, $\upsilon_{C=O}$ 1689 cm^{-1}; ES-MS (m/z) calcd. for $C_{23}H_{29}N_2O_5$: 413.0 $(M + H)^+$; found 413.

3,5-Diphenyl-1*H*-pyrrole-2-carboxylic acid ethyl ester (1a). Compound **3a** (10 g, 29 mmol) was dissolved in dry ethanol (50 mL), treated with formamidine sulfinic acid (10 g, 92 mmol) and the suspension was heated under reflux under nitrogen for 14 hours. The reaction mixture was allowed to cool to room temperature and the solvent was evaporated to a brown residue. Recrystallisation from ethanol gave the product **1a** as a crystalline solid (3.32 g, 39%), m.p. 139–140 °C (lit. m.p. 138–139 °C).[26] ^{1}H NMR (300 MHz, $CDCl_3$) δ: 9.51 (bs, 1H), 7.57–7.62 (m, 4H), 7.28–7.44 (m, 6H), 6.61 (d, 1H, $J = 3.0$ Hz), 4.26 (q, $J = 7.2$ Hz, 2H), 1.23 (t, $J = 7.2$ Hz, 3H); ^{13}C NMR (75 MHz, $CDCl_3$) δ: 161.6, 135.7, 135.4, 133.7, 131.4, 129.8, 129.3, 128.1, 127.9, 127.3, 125.1, 118.9, 110.2, 60.6, 14.4; IR (KBr disc): υ_{N-H} 3313, $\upsilon_{C=O}$ 1662 cm^{-1}; UV-visible (EtOH): λ_{max} = 263, 308 nm; ES-MS (m/z) calcd. for $C_{19}H_{17}NO_2$: 292.0 $(M + H)^+$; found: 292.1; Anal. calcd. for $C_{19}H_{17}NO_2$: C, 78.33; H, 5.88; N, 4.81; found C, 78.41; H, 5.89; N, 4.79%.

3-(4-Dimethylaminophenyl)-5-phenyl-1*H*-pyrrole-2-carboxylic acid ethyl ester (1b). Compound **3b** (10 g, 26 mmol) was dissolved in dry ethanol (100 mL), treated with formamidine sulfinic acid (9.5 g, 88 mmol) and the suspension was heated under reflux under nitrogen for 14 hours. The mixture was allowed to cool to room temperature and the solvent was evaporated to a brown residue. Recrystallisation from ethanol gave the product **1b** as a crystalline solid (3.4 g, 39%), m.p. 135–137 °C. ^{1}H NMR (300 MHz, $CDCl_3$) δ: 9.34 (bs, 1H), 7.51–7.61 (m, 4H), 7.38–7.43 (m, 2H), 7.27–7.32 (m, 1H), 6.74–6.79

(m, 2H), 6.59 (d, 1H, $J = 3.08$), 4.29 (q, 2H, $J = 7.2$ Hz), 2.98 (s, 6H), 1.29 (t, 3H, $J = 7.2$ Hz); ^{13}C NMR (75 MHz, $CDCl_3$) δ: 161.6, 150.1, 135.5, 134.2, 131.6, 130.5, 129.2, 128.0, 125.0, 123.4, 118.3, 112.1, 109.8, 60.4, 40.9, 14.6; IR (KBr disc): υ_{N-H} 3342, $\upsilon_{C=O}$ 1664 cm^{-1}; UV-visible (EtOH): $\lambda_{max} = 294$ nm; ES-MS (m/z) calcd. for $C_{21}H_{22}N_2O$: 335.0 $(M + H)^+$; found: 335.1; Anal. calcd. for $C_{21}H_{22}N_2O_2$: C, 75.42; H, 6.63; N, 8.38; found C, 75.41; H, 6.62; N, 8.26%.

3-(4-Dimethylamino-2,6-dimethylphenyl)-5-phenyl-1*H*-pyrrole-2-carboxylic acid ethyl ester (1c). (4-Dimethylamino-2,6-dimethylphenyl)-2-nitro-5-oxo-5-phenylpentanoic acid ethyl ester **3c** (1 g, 2.4 mmol) was dissolved in dry ethanol (40 mL), treated with formamidine sulfinic acid (1.05 g, 9.7 mmol) and the suspension was heated under reflux under nitrogen for 24 hours. The mixture was allowed to cool to room temperature and the solvent was evaporated to a brown residue. Recrystallisation from ethanol gave the product **1c** as a yellow coloured crystalline solid (0.2 g, 22%), mp 157–160 °C. ^{1}H NMR (300 MHz, $CDCl_3$) δ: 9.59 (bs, 1H), 7.60–7.63 (m, 2H), 7.38–7.43 (m, 2H), 7.26–7.31 (m, 1H), 6.52 (s, 2H), 6.41 (d, $J =$ 2.8 Hz, 1H), 4.13 (q, $J = 7.1$ Hz, 2H), 2.94 (s, 6H), 2.09 (s, 6H), 1.07 (t, $J = 7.1$ Hz, 3H); ^{13}C NMR (75 MHz, $CDCl_3$) δ: 161.6, 149.7, 137.3, 135.5, 132.0, 131.5, 129.0, 127.6, 124.7, 124.5, 120.2, 111.6, 110.5, 59.9, 40.9, 21.3, 14.1; IR (KBr disc): υ_{N-H} 3328, $\upsilon_{C=O}$ 1677 cm^{-1}; UV-visible (EtOH): $\lambda_{max} = 307$ nm; ES-MS (m/z) calcd. for $C_{23}H_{26}N_2$: 363.0 $(M + H)^+$; found: 363.2; Anal. calcd. for $C_{23}H_{26}N_2$: C, 76.21; H, 7.23; N, 7.73; found C, 75.99; H, 7.30; N, 7.79%.

X-Ray data collection, structure solution and refinement

Data were collected on a Siemens-Bruker P4 diffractometer for the structures **1a** and **1b** at room temperature (294 K) and processed using the XSCANS suite of programs.[27] A study at 294 K of **1c** has been deposited with the CSD as 233395† but has not been referred to in the text. A low-temperature study was undertaken of **1c** at 150 K using a Bruker APEX diffractometer and data were processed using the SMART suite of programs.[28] Mo-Kα radiation (0.71073 Å) was used in all structural studies with graphite monochromator. Compound **1a** crystallizes in the monoclinic system, space group $P2_1/c$ (No. 14) ($Z' = 1$) while both derivatives **1b** ($Z' = 2$, two independent molecules A and B per asymmetric unit) and **1c** ($Z' = 1$) crystallize in the triclinic system ($P\bar{1}$, No. 2). Solution and refinement was undertaken using SHELXS97 and SHELXL97.[29] The graphics were generated with ORTEX[30] and PLATON.[31]

No disorder is present in **1a**, but in the asymmetric unit of **1b** a minor component of rotational disorder was detected in three of the methyl groups in the two Me_2N moieties of the independent A and B molecules. These were treated accordingly by using six partial occupancy H atom sites with AFIX 127 in SHELXL97 to give site occupancies of 0.81 : 0.19, 0.74 : 0.26 and 0.88 : 0.12. Data for **1c** were collected on a Bruker APEX CCD diffractometer at 150 K. Carboxylate disorder is observed in **1c** but with site occupancy factors of 0.608(4) and 0.392(4) for the major and minor orientations, respectively, and one of the methyl groups C37 has rotational disorder with respect to the three hydrogen atoms resulting in major : minor orientations of 0.61(2) and 0.39(2).

All non hydrogen atoms were refined using anisotropic displacement parameters and hydrogen atoms were treated as riding atoms using the SHELXL97 defaults at the appropriate temperature whereas the N–H hydrogen atoms were refined with isotropic displacement parameters. The carboxylate disorder in **1c** was treated using appropriate soft DFIX/DELU/ISOR restraints in the final cycles of full matrix least squares refinement: the rotational disorder in the methyl groups of **1c** was treated using the AFIX 127 command in SHELXL97.

Crystallographic data

1a, Chemical formula $C_{19}H_{17}NO_2$, colourless, molecular weight 291.34 g mol^{-1}, monoclinic, space group $P2_1/c$ (No. 14), $a = 10.5232(12)$, $b = 7.5048(4)$, $c = 20.2461(15)$ Å, $\beta = 102.020(7)°$, $V = 1563.9(2)$ Å^3, $Z = 4$, $T = 294(1)$ K, density = 1.237 g cm^{-3} (calc.), $F(000) = 616$, $\mu = 0.080$ mm^{-1}, 4173 reflections to $2\theta = 52°$, 3081 unique (with 2189 $I > 2\sigma I$), 204 parameters, R-factor is 0.045, $wR_2 = 0.102$ (based on F^2 for with $I > 2\sigma I$) using SHELXL97, $Gof = 1.03$, density range in final Δmap is -0.19 to $+0.21$ e. Å^{-3}.

1b, Chemical formula $C_{21}H_{22}N_2O_2$, colourless, molecular weight 334.41 g mol^{-1}, triclinic, space group $P\bar{1}$ (No. 2), $a =$ 9.8173(11), $b = 13.3363(11)$, $c = 15.9016(10)$ Å, $\alpha = 67.237(5)°$, $\beta = 80.480(8)°$, $\gamma = 72.421(8)°$, $V = 1827.3(3)$ Å^3, $Z = 4$, $T =$ 294(1) K, density = 1.216 g cm^{-3} (calc.), $F(000) = 712$, $\mu =$ 0.079 mm^{-1}, 8324 reflections to $2\theta = 52°$, 7032 unique (with 4257 $I > 2\sigma I$), 468 parameters, R-factor is 0.054, $wR_2 = 0.119$ (based on F^2 for with $I > 2\sigma I$) using SHELXL97, $Gof = 1.03$, density range in final Δmap is -0.32 to $+0.34$ e. Å^{-3}.

1c, Chemical formula $C_{23}H_{26}N_2O_2$, yellow, molecular weight 362.46 g mol^{-1}, triclinic, space group $P\bar{1}$ (No. 2), $a =$ 7.6973(5), $b = 9.3729(6)$, $c = 14.0807(10)$ Å, $\alpha = 83.347(1)°$, $\beta = 82.391(1)°$, $\gamma = 79.132(1)°$, $V = 984.54(11)$ Å^3, $Z = 2$, $T = 150(2)$ K, density = 1.223 g cm^{-3} (calc.), $F(000) = 388$, $\mu = 0.078$ mm^{-1}, 16869 reflections to $2\theta = 56.5°$, 4591 unique (with 3988 $I > 2\sigma I$), 274 parameters, R-factor is 0.048, $wR_2 =$ 0.127, (based on F^2 for with $I > 2\sigma I$) using SHELXL97, $Gof =$ 1.04, density range in final Δmap is -0.28 to $+0.28$ e. Å^{-3}.

Crystallographic data (excluding structure factors) for **1a–c** have been deposited with the Cambridge Crystallographic Data Centre.†

UV-visible and fluorescence procedures

Solvents used were spectrophotometric grade chloroform, which was distilled over potassium carbonate prior to use, spectrophotometric grade acetonitrile and HPLC grade cyclohexane. Stock solutions (5×10^{-5} M) of each diarylpyrrole ester **1a–c** were prepared in chloroform. For UV-visible analysis a 1 in 10 dilution from the stock solution into cyclohexane and acetonitrile was performed to give solutions of 5×10^{-6} M concentration. In all cases the UV-visible spectra were determined from a 1 cm path quartz cell at room temperature. Baseline corrected UV-visible spectra were collected between 250 and 500 nm. All UV-visible spectra were normalised to 1 at their position of maximum absorbance. For fluorescence analysis the respective 5×10^{-6} M UV-visible solutions were diluted by a factor of 10 with acetonitrile and cyclohexane to give solutions of 5×10^{-7} M concentration. In all cases fluorescence was determined at room temperature from a 1 cm path quartz cell with excitation and emission slit widths of 5 nm and a PMT detector voltage of 600 volts. Baseline corrected fluorescence spectra for **1a–b** were obtained by exciting solutions at 285 nm and collecting the fluorescence between 295 and 600 nm. Baseline correction for the poorly emitting **1c** did not give satisfactory spectra. Therefore in order to avoid 2nd order solvent scattering interference for **1c**, the solutions were excited at 310 nm and the fluorescence collected between 320 and 600 nm. All fluorescence spectra were normalised to 1 at their position of maximum emission.

† CCDC reference numbers 233393–233396. See http://dx.doi.org/10.1039/b507669b for crystallographic data in CIF or other electronic format.

Acknowledgements

This work was funded under the Program for Research in Third-Level Institutions administered by the HEA. J. F. G. thanks Dublin City University for the purchase of a Siemens P4 diffractometer and computer system. Thanks to Dr D. Rai of the CSCB Mass Spectrometry Centre for mass analyses and Dr H. Mueller-Bunz of the UCD Crystallographic Centre for collecting a low temperature dataset for **1c**.

References

1 A. P. de Silva, H. Q. N. Gunaratne, T. Gunnlaugsson, A. J. M. Huxley, C. P. McCoy, J. T. Rademacher and T. E. Rice, *Chem. Rev*., 1997, **97**, 1515.
2 R. P. Haugland, in *Handbook of Fluorescent Probes and Research Products*, 10th edn, ed. M. T. Z. Spence, 2005, Molecular Probes, Eugene, OR, USA.
3 (*a*) K. Rurack and U. Resch-Genger, *Chem. Soc. Rev*., 2002, **31**, 116; (*b*) B. Valeur, *Topics in Fluorescence Spectroscopy Probe Design and Chemical Sensing*, ed. J. R. Lakowicz, Plenum, New York, 1994, vol. **4**, 21; (*c*) R. A. Bissell, A. P. de Silva, H. Q. N. Gunaratne, P. L. M. Lynch, G. E. M. Maguire and K. R. A. Sandanayake, *Chem. Soc. Rev*., 1992, **187**.
4 For examples see: (*a*) T. Gunnlaugsson, A. P. Davis, G. M. Hussey, J. Tierney and M. Glynn, *Org. Biomol Chem*., 2004, **2**, 1856; (*b*) L. M. Daffy, A. P. de Silva, H. Q. N. Gunaratne, C. Huber, P. L. M. Lynch, T. Werner and O. S. Wolfbeis, *Chem. Eur. J*., 1998, **4**, 1180; (*c*) C. J. Fahrni, L. Yang and D. G. VanDerveer, *J. Am. Chem. Soc*., 2003, **125**, 3799.
5 For examples see: (*a*) K. Rurack, M. Kollmannsberger, U. Resch-Genger and J. Daub, *New J. Chem*., 2001, **25**, 289; (*b*) T. Hirano, K. Kikuchi, Y. Urano, T. Higuchi and T. Nagano, *J. Am. Chem. Soc*., 2000, **122**, 12399; (*c*) S. A. Jonker, S. I. Van Dijk, K. Goubitz, C. A. Reiss, W. Schuddeboom and J. W. Verhoeven, *Mol. Cryst. Liq. Cryst*., 1990, **183**, 273.
6 For example: (*a*) J. F. Callan, A. P. deSilva, J. Ferguson, A. J. M. Huxley and A. M. O'Brien, *Tetrahedron*, 2004, **60**, 11125; (*b*) K. Rurack, A. Danel, K. Rotkiewicz, D. Grabka, M. Spieles and W. Rettig, *Org. Lett*., 2002, **4**, 4647.
7 (*a*) J. Killoran, L. Allen, J. F. Gallagher, W. M. Gallagher and D. F. O'Shea, *Chem. Commun*., 2002, 1862; (*b*) A. Gorman, J. Killoran, C. O'Shea, T. Kenna, W. M. Gallagher and D. F. O'Shea, *J. Am. Chem. Soc*., 2004, **126**, 10619; (*c*) W. M. Gallagher, L. T. Allen, C. O'Shea, T. Kenna, M. Hall, A. Gorman, J. Killoran and D. F. O'Shea, *Br. J. Cancer*, 2005, **92**, 1702.
8 X. Fan and Y. Zhang, *Tetrahedron Lett*., 2002, **43**, 1863.
9 M. Nitta and T. Kobayashi, *Chem. Lett*., 1983, **1715**.
10 L. W. Deady, *Tetrahedron*, 1967, **23**, 3505.
11 E. M. Campi, G. D. Fallon, W. R. Jackson and Y. Nilsson, *Aust. J. Chem*., 1992, **45**, 1167.
12 S. L. Buchwald, M. W. Wannamaker and B. T. Watson, *J. Am. Chem. Soc*., 1989, **111**, 776.
13 B. Quiclet-Sire, I. Thévenot and S. Z. Zard, *Tetrahedron Lett*., 1995, **36**, 9469.
14 G. R. Desiraju and T. Steiner, *The Weak Hydrogen Bond in Structural Chemistry and Biology*, Oxford University Press, New York, 1999.
15 (*a*) J. F. Malone, C. M. Murray, M. H. Charlton, R. Docherty and A. J. Lavery, *J. Chem. Soc., Faraday Trans*., 1997, **93**, 3429; (*b*) W. B. Jennings, B. M. Farrell and J. F. Malone, *Acc. Chem. Res*., 2001, **34**, 885.
16 J. Bernstein, R. E. Davis, L. Shimoni and N. L. Chang, *Angew. Chem. Int. Ed*., 1995, **34**, 1555.
17 (*a*) V. Bennis and J. F. Gallagher, *Acta Crystallogr, Sect. C: Cryst. Struct. Commun*., 1998, **C54**, 477; (*b*) J. F. Gallagher and E. M. Moriarty, *Acta Crystallogr, Sect. C: Cryst. Struct. Commun*., 1999, **C55**, 1079.
18 F. H. Allen, *Acta Crystallogr., Sect. B: Struct. Sci*., 2002, **B58**, 380.
19 H. Takaya, S. Kojima and S. I. Murahashi, *Org. Lett*., 2001, **3**, 421.
20 (*a*) S. Techert, S. Schmatz, A. Wiessner and H. Staerk, *J. Phys. Chem. A*, 2000, **104**, 5700; (*b*) Z. R. Grabowski, K. Rotkiewicz and W. Rettig, *Chem. Rev*., 2003, **103**, 3899.
21 C. Cornelissen-Gude and W. Rettig, *J. Phys. Chem. A*, 1998, **102**, 7754.
22 (*a*) F. Mohamadi, N. G. J. Richards, W. C. Guida, R. Liskamp, M. Lipton, C. Caufield, G. Chang, T. Hendrickson and W. C. Still, *J. Comput. Chem*., 1990, **112**, 6127; (*b*) W. C. Still, A. Tempczyk, R. C. Hawley and T. Hendrickson, *J. Am. Chem. Soc*., 1990, **112**, 6127.
23 Ch. Grundmann and J. M. Dean, *Angew. Chem., Int. Ed. Engl*., 1965, **4**, 955.
24 N. L. Silver and D. W. Boykin Jr., *J. Org. Chem*., 1970, **35**, 759.
25 W. Davey and D. J. Tivey, *J. Chem. Soc*., 1958, **2276**.
26 (*a*) I. Fejes, L. Toke, G. Blaskó, M. Nyerges and C. S. Pak, *Tetrahedron*, 2000, **56**, 8545; (*b*) M. W. L. Chung and M. P. Sammes, *J. Chem. Res*., 1987, 292.
27 Siemens Bruker AXS 1994, XSCANS Software, Ver. 2.2 Madison, Wisconsin, U.S.A.
28 Bruker 2000 SMART, *SAINT and SADABS*, Bruker AXS Inc., Madison, Wisconsin, U.S.A.
29 G. M. Sheldrick, *SHELXL-97, Program for refinement of crystal structures*, University of Göttingen, Germany, 1997G. M. Sheldrick, *SHELXS-97, Program for solution of crystal structures*, University of Göttingen, Germany, 1997.
30 P. McArdle, *J. Appl. Cryst*., 1995, **28**, 65.
31 A. L. Spek, *J. Appl. Cryst*., 2003, **36**, 7.